

## Microwave Magnetochiral Dichroism in the Chiral-Lattice Magnet $\text{Cu}_2\text{OSeO}_3$

Y. Okamura,<sup>1</sup> F. Kagawa,<sup>2</sup> S. Seki,<sup>2,3</sup> M. Kubota,<sup>2,4,\*</sup> M. Kawasaki,<sup>1,2</sup> and Y. Tokura<sup>1,2</sup>

<sup>1</sup>*Department of Applied Physics and Quantum Phase Electronics Center, University of Tokyo, Tokyo 113-8656, Japan*

<sup>2</sup>*RIKEN Center for Emergent Matter Science (CEMS), Wako 351-0198, Japan*

<sup>3</sup>*PRESTO, Japan Science and Technology Agency, Bunkyo, Tokyo 113-8656, Japan*

<sup>4</sup>*Research and Development Headquarters, ROHM Co., Ltd., Kyoto 615-8585, Japan*

(Received 16 January 2015; revised manuscript received 27 March 2015; published 12 May 2015)

Through broadband microwave spectroscopy in Faraday geometry, we observe distinct absorption spectra accompanying magnetolectric (ME) resonance for oppositely propagating microwaves, i.e., directional dichroism, in the multiferroic chiral-lattice magnet  $\text{Cu}_2\text{OSeO}_3$ . The magnitude of the directional dichroism critically depends on the magnetic-field direction. Such behavior is well accounted for by considering the relative direction of the oscillating electric polarizations induced via the ME effect with respect to microwave electric fields. Directional dichroism in a system with an arbitrary form of ME coupling can be also discussed in the same manner.

DOI: 10.1103/PhysRevLett.114.197202

PACS numbers: 75.85.+t, 75.30.Ds, 76.50.+g, 85.75.-d

Multiferroics, in which magnetic and ferroelectric orders coexist and are strongly coupled with each other, form a promising class of materials that is capable of efficient mutual control of magnetization ( $\mathbf{M}$ ) and electric polarization ( $\mathbf{P}$ ) [1–4]. In fact, the strong magnetolectric (ME) coupling in multiferroics results in various ME responses against dc external fields, such as the magnetic-field control of the  $\mathbf{P}$  direction and the electric-field control of the spin chirality, magnetic domain, and  $\mathbf{M}$  direction [5–7].

Magnetic and ferroelectric properties in multiferroics may also be entangled in a finite-frequency regime, and the ME response may even be resonantly enhanced. Such a resonant mode of dynamical ME response is equivalent to collective spin excitations that are electric-dipole active; thus, it is often called an electromagnon and is now ubiquitously found in multiferroics in a gigahertz-to-terahertz frequency range [8–10]. As a result of the resonantly enhanced ME coupling, electromagnon excitation is often accompanied by a salient optical response, i.e., directional dichroism; at the resonance frequency, the material shows a different absorption or transmittance for oppositely propagating, linearly polarized light. Experimental realizations of directional dichroism via electromagnons have been reported in recent years [11–17], and remarkably, some materials exhibit a large difference in the transmission coefficient ( $\sim 400\%$ ) for oppositely propagating light [15,17].

However, experimental observations of directional dichroism are still rather rare, and in particular it is currently difficult to predict the configuration where the largest directional dichroism will be realized in a given material. In this context, thus far, a phenomenological quantity,  $\mathbf{k}^\omega \cdot (\mathbf{P} \times \mathbf{M})$ , where  $\mathbf{k}^\omega$  denotes the propagation direction of light or microwave and the vector product  $\mathbf{P} \times \mathbf{M}$  ensures the existence of a macroscopic toroidal moment [18], has

often been introduced and employed to explain the presence or absence of directional dichroism, in particular in Voigt geometry [14]. This  $\mathbf{k}^\omega \cdot (\mathbf{P} \times \mathbf{M})$  description, however, obviously collapses when considering directional dichroism in Faraday geometry ( $\mathbf{k}^\omega \parallel \mathbf{M}$ ); while  $\mathbf{k}^\omega \cdot (\mathbf{P} \times \mathbf{M})$  always results in a zero value in Faraday geometry by definition, directional dichroism should be allowed, for instance, when time-reversal symmetry is broken in a chiral crystal [19]. This inadequacy of the  $\mathbf{k}^\omega \cdot (\mathbf{P} \times \mathbf{M})$  framework suggests that the dynamics of  $\mathbf{P}$  and  $\mathbf{M}$  under microwave irradiation should be taken into account, rather than the static  $\mathbf{P}$  and  $\mathbf{M}$ , to describe directional dichroism under arbitrary geometries. In this Letter, through broadband microwave spectroscopy in various Faraday geometries ( $\mathbf{k}^\omega \parallel \mathbf{H}$ ) in the chiral-lattice multiferroic  $\text{Cu}_2\text{OSeO}_3$ , we successfully observe directional dichroism. Our comprehensive experimental study clarifies that the behavior of the directional dichroism accompanying ME resonance is well accounted for by considering the static ME coupling of the system. This microscopic insight into the directional dichroism can be applied to a system with arbitrary ME coupling, thereby giving a guideline for how to achieve the largest directional dichroism in a given material.

The title compound  $\text{Cu}_2\text{OSeO}_3$  belongs to the chiral cubic space group  $P2_13$  [20–23], and spin-1/2 local moments residing at the  $\text{Cu}^{2+}$  ions form various magnetically ordered states below  $T_c \approx 58$  K, depending on the applied magnetic fields: at a zero magnetic field, a proper-screw type, helical spin structure is realized; as the magnetic field increases, the helical spin structure turns into a ferrimagnetic state through a conical state and in a specific temperature range (55–58 K) through a Skyrmion crystal state [22]. These magnetic orderings in addition to the original chiral-crystal symmetry endow the material with various ME properties depending on the magnetic-field direction; for instance,  $\mathbf{P}$  appears

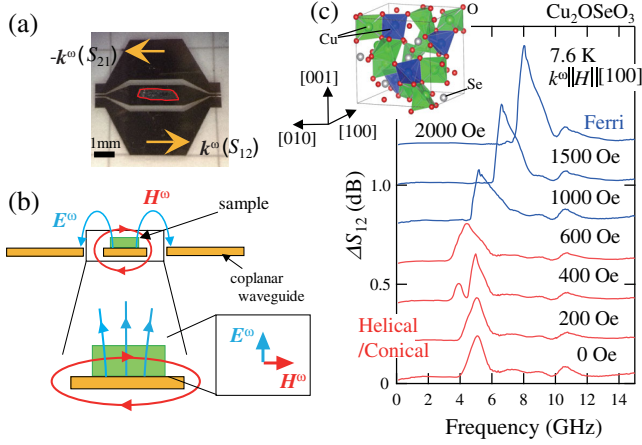


FIG. 1 (color online). (a) Picture of the experimental setup. The sample is mounted on the coplanar waveguide (CPW) directly. The sample shape is highlighted by the red line for clarity.  $S_{12(21)}$  is the transmission coefficient for the microwave propagating along the  $+k^\omega$  ( $-k^\omega$ ) direction. (b) Schematic of the electromagnetic-field distribution  $E^\omega$  and  $H^\omega$  accompanying the microwave propagating along the CPW. (c) The absorption spectra associated with the magnetic resonance,  $\Delta S_{12}$ , at various magnetic fields with the  $k^\omega \parallel H \parallel [100]$  configuration at 7.6 K. Each spectrum is shifted vertically for clarity. Inset: the crystal structure of  $\text{Cu}_2\text{OSeO}_3$ .

along the [001] axis when  $H$  is applied along the [110] axis, whereas  $P$  does not appear when  $H$  is along the [001] axis [20–22,24].

Single crystals of  $\text{Cu}_2\text{OSeO}_3$  were grown by chemical vapor transport [22]. We performed broadband microwave spectroscopy to measure the transmission coefficient of the sample mounted on a coplanar waveguide (CPW). The transmission coefficient for a microwave propagating along the  $+k^\omega$  and  $-k^\omega$  directions is denoted as  $S_{12}$  and  $S_{21}$ , respectively, and was recorded with a vector network analyzer (Agilent Technology, E8363C). The absorption spectrum associated with the electromagnon excitations, denoted as  $\Delta S_{12}$  (or  $\Delta S_{21}$ ) for the  $+k^\omega$  (or  $-k^\omega$ ) microwave, was obtained by calculating  $\Delta S_{12(21)} = -S_{12(21)}(H) + S_{12(21)}(H_{\text{ref}})$ , where  $S_{12(21)}(H_{\text{ref}})$  was taken at a magnetic field  $H_{\text{ref}}$  such that the magnetic resonance of interest does not appear in the experimental frequency window (0.1–15 GHz): in the present case,  $H_{\text{ref}} = 5000$  Oe was chosen (for more details, see the Supplemental Material [25]). The width of the signal line is designed to be 1 mm [Fig. 1(a)], which is wider than the sample width ( $\approx 0.5$  mm), so that the oscillating magnetic field  $H^\omega$  and oscillating electric field  $E^\omega$  at the sample position can be approximated as parallel and perpendicular to the substrate, respectively [Fig. 1(b)]. Figure 1(c) shows the microwave transmission spectra under various magnetic fields with the  $k^\omega \parallel H \parallel [100]$  configuration. The resonance peak is observed around 5 GHz at a zero field and shifts systematically as the magnetic field increases.

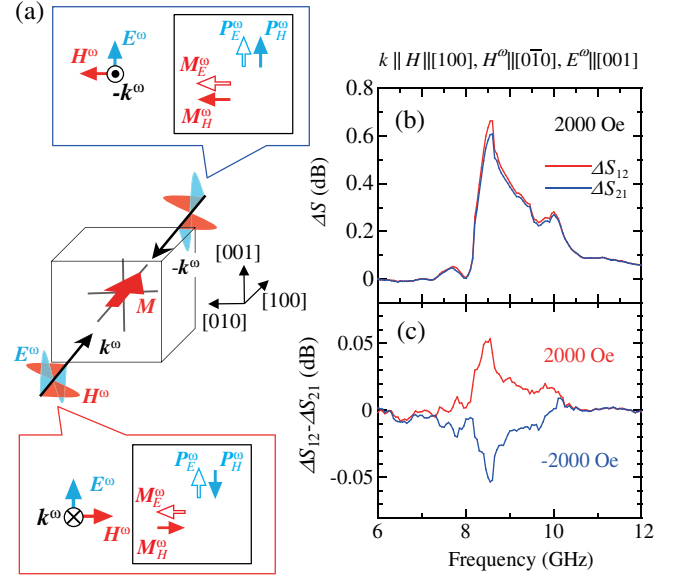


FIG. 2 (color online). (a) Measurement configuration and the instantaneous responses of  $M^\omega$  and  $P^\omega$  derived from the  $d$ - $p$  hybridization model for the case that  $M \parallel [100]$  with  $E^\omega \parallel [001]$  and  $H^\omega \parallel [0\bar{1}0]$ .  $M^\omega$  and  $P^\omega$  induced by  $E^\omega$  are denoted as  $M_E^\omega$  (open red arrows) and  $P_E^\omega$  (open blue arrows), respectively, whereas  $M^\omega$  and  $P^\omega$  induced by  $H^\omega$  are denoted as  $M_H^\omega$  (filled red arrows) and  $P_H^\omega$  (filled blue arrows), respectively. (b) The absorption spectra  $\Delta S_{12}$  and  $\Delta S_{21}$  under 2000 Oe for  $k^\omega \parallel [100]$  and  $k^\omega \parallel [\bar{1}00]$ , respectively. (c) The directional-dichroism spectra  $\Delta S_{12} - \Delta S_{21}$  under  $\pm 2000$  Oe. The measurements were performed at 7.8 K.

These behaviors reproduce well previous results [26] and are in good agreement with a theoretical model [27].

We first look into the directional-dichroism spectrum for  $k^\omega \parallel [100]$  at 2000 Oe, where the magnetic state is ferromagnetic [Fig. 2(a)]. As mentioned above, directional dichroism in Faraday geometry can be expected irrespective of the magnetic structure in  $\text{Cu}_2\text{OSeO}_3$  because of the crystal chirality and the broken time-reversal symmetry under a magnetic field. In fact, we found a clear signature of directional dichroism, i.e., the resonance peak at  $\sim 8$  GHz is slightly higher in the  $\Delta S_{12}$  spectrum than in the  $\Delta S_{21}$  spectrum [Fig. 2(b)]: the nonreciprocal nature can be better discerned when the  $\Delta S_{12} - \Delta S_{21}$  spectrum is derived, as displayed in Fig. 2(c). To verify the nonreciprocal nature further, we also measured the  $\Delta S_{12} - \Delta S_{21}$  spectrum in the inverted magnetic field,  $-2000$  Oe, because the nonreciprocal signal is expected to be reversed by the time-reversal operation. In fact, the sign reversal in the  $\Delta S_{12} - \Delta S_{21}$  spectrum was clearly observed [Fig. 2(c)], as expected.

To understand the directional dichroism at a more microscopic level, we consider the microwave-induced dynamics of  $P$  and  $M$ . In the presence of ME coupling, the oscillating components  $P^\omega$  and  $M^\omega$  are approximated by a sum of two contributions from distinct microscopic origins:

$$P^\omega = \epsilon_0 \chi^{\leftrightarrow ee}(\omega) E^\omega + \sqrt{\epsilon_0 \mu_0} \chi^{\leftrightarrow em}(\omega) H^\omega \equiv P_E^\omega + P_H^\omega, \quad (1)$$

$$\mathbf{M}^\omega = \sqrt{\frac{\epsilon_0}{\mu_0}} \chi^{\leftrightarrow \text{me}}(\omega) \mathbf{E}^\omega + \mu_0 \chi^{\leftrightarrow \text{mm}}(\omega) \mathbf{H}^\omega \equiv \mathbf{M}_E^\omega + \mathbf{M}_H^\omega, \quad (2)$$

where  $\chi^{\leftrightarrow \text{ee}}$ ,  $\chi^{\leftrightarrow \text{mm}}$ , and  $\chi^{\leftrightarrow \text{em(me)}}$  are the dynamical dielectric tensor, dynamical magnetic tensor [28], and dynamical ME tensors, respectively, as a function of frequency  $\omega$ . While the microwave- $\mathbf{E}^\omega$ -induced  $\mathbf{P}_E^\omega$  is parallel to  $\mathbf{E}^\omega$  when  $\mathbf{E}^\omega$  is applied along one of the principal axes, the microwave- $\mathbf{H}^\omega$ -induced  $\mathbf{P}_H^\omega$  can be directed to any direction according to the dynamical ME tensor of a compound; nevertheless, the direction of  $\mathbf{P}_H^\omega$  in a microwave regime can be deduced from, in the zeroth-order approximation, the feature of the static ME coupling. We note that the static ME coupling in  $\text{Cu}_2\text{OSeO}_3$  is well described by the  $d$ - $p$  hybridization model. According to Ref. [22], a magnetic-field-dependent part of the electric polarization  $\Delta \mathbf{P}$  can be approximately given as

$$\Delta \mathbf{P} = \lambda (M_{[010]} M_{[001]}, M_{[100]} M_{[001]}, M_{[100]} M_{[010]}), \quad (3)$$

where  $\lambda$  is a coupling constant,  $M_{[100]}$  denotes the [100] component of the magnetization, and so on [22,24,29–32]. For instance, we consider a situation where the static  $\mathbf{H}$  (and thus  $\mathbf{M}$ ) is along [100]. When a magnetic resonance is excited by irradiating the microwave  $\mathbf{H}^\omega$  along [010], the resonant mode produces a resonantly enhanced  $\mathbf{M}_H^\omega$  ( $\parallel [010]$ ) by definition. In the present system,  $\mathbf{M}_H^\omega$  also induces a resonantly enhanced  $\mathbf{P}_H^\omega$  along [001] through the ME coupling given by Eq. (3), as a manifestation of the resonantly enhanced  $\chi^{\leftrightarrow \text{em}}$ . Below, we consider the case where  $\mathbf{P}_H^\omega$  is resonantly enhanced and see its vital role in the directional dichroism.

In Fig. 2(a), we illustrate the instantaneous responses of  $\mathbf{P}_H^\omega$ ,  $\mathbf{P}_E^\omega$ ,  $\mathbf{M}_H^\omega$ , and  $\mathbf{M}_E^\omega$  in Faraday geometry under microwave irradiation with  $\mathbf{k}^\omega \parallel [100]$  (bottom panel) and  $-\mathbf{k}^\omega \parallel [100]$  (top panel). Note that while  $\mathbf{P}_E^\omega$  is always parallel to  $\mathbf{E}^\omega$  irrespective of  $\pm \mathbf{k}^\omega$ ,  $\mathbf{P}_H^\omega$  can be either parallel or antiparallel to  $\mathbf{E}^\omega$ ; consequently, the magnitude of the total  $\mathbf{P}^\omega (= \mathbf{P}_E^\omega + \mathbf{P}_H^\omega)$  depends on  $\pm \mathbf{k}^\omega$ , rationalizing the  $\pm \mathbf{k}^\omega$ -dependent microwave absorption. Furthermore, the parallel or antiparallel relationship between  $\mathbf{P}_H^\omega$  and  $\mathbf{P}_E^\omega$  is reversed when the external magnetic fields are inverted, which is also consistent with the sign reversal of the directional dichroism [Fig. 2(c)].

The directional dichroism in other experimental geometries is also well accounted for by considering the interference between  $\mathbf{P}_H^\omega$  and  $\mathbf{P}_E^\omega$ , or equivalently, by considering the relative direction of  $\mathbf{P}_H^\omega$  with respect to  $\mathbf{E}^\omega$ . Figures 3(a)–3(c) illustrate various Faraday geometries, and the corresponding absorption spectra with one and the same piece are displayed in Figs. 3(d)–3(f). The relative direction of  $\mathbf{P}_H^\omega$  with respect to  $\mathbf{E}^\omega$  is readily derived for each configuration by employing Eq. (1), and

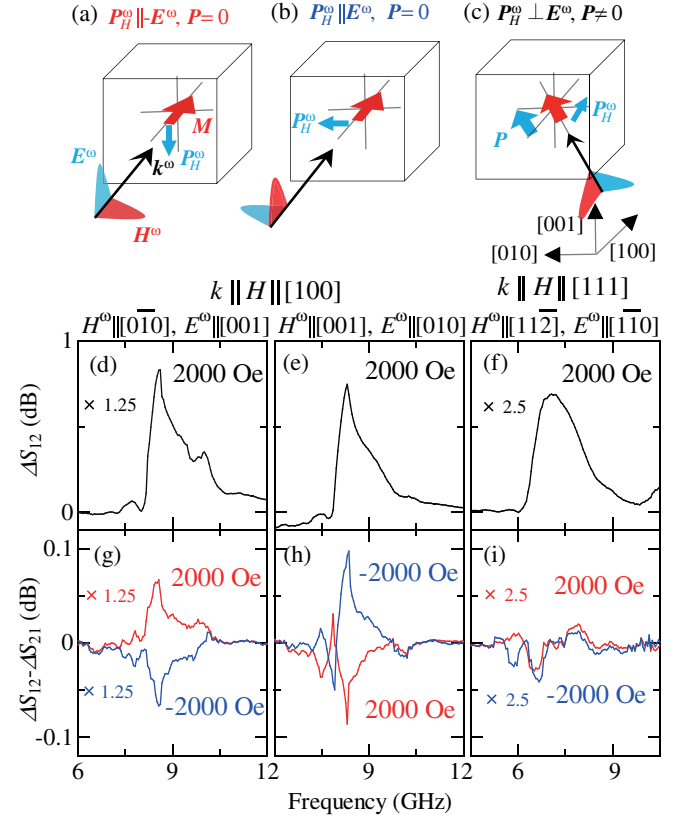


FIG. 3 (color online). (a)–(c) Schematics of the experimental configurations for (a)  $\mathbf{k}^\omega \parallel \mathbf{H} \parallel [100]$ ,  $\mathbf{H}^\omega \parallel [0\bar{1}0]$ , and  $\mathbf{E}^\omega \parallel [001]$ , (b)  $\mathbf{k}^\omega \parallel \mathbf{H} \parallel [100]$ ,  $\mathbf{H}^\omega \parallel [001]$ , and  $\mathbf{E}^\omega \parallel [010]$ , and (c)  $\mathbf{k}^\omega \parallel \mathbf{H} \parallel [111]$ ,  $\mathbf{H}^\omega \parallel [11\bar{2}]$ , and  $\mathbf{E}^\omega \parallel [1\bar{1}0]$ . (d)–(f) The absorption spectra  $\Delta S_{12}$  at 2000 Oe under the microwave configuration of (a)–(c), respectively. (g)–(i) The directional dichroism spectra  $\Delta S_{12} - \Delta S_{21}$  at  $\pm 2000$  Oe under the microwave configuration of (a)–(c), respectively. The measurements were performed at 7.6 K.

it is antiparallel, parallel, and perpendicular for the configurations of Figs. 3(a), 3(b), and 3(c), respectively. Note that the sign of the directional dichroism is inverted between Figs. 3(g) and 3(h) and that the directional dichroism almost vanishes in Fig. 3(i). Furthermore, we also confirmed that in the  $\mathbf{k}^\omega \parallel [110]$ ,  $\mathbf{H}^\omega \parallel [1\bar{1}0]$ , and  $\mathbf{E}^\omega \parallel [001]$  configuration, in which  $\mathbf{P}_H^\omega$  is not induced within the framework of Eq. (1), the directional dichroism is negligibly small (not shown). Thus, the variation in the directional dichroism magnitude is in good agreement with the manner of the interference between the microwave- $\mathbf{E}^\omega$ -induced  $\mathbf{P}_E^\omega$  and the microwave- $\mathbf{H}^\omega$ -induced  $\mathbf{P}_H^\omega$ . Parasitic fine structures adjacent to the main peak in Fig. 3(h) currently remain to be explained and may be ascribed to a so-called spin-wave resonance [33]. We note that the same scheme is applicable to the Voigt geometry as well: in the  $\mathbf{k}^\omega \parallel [110]$ ,  $\mathbf{H}^\omega \parallel [001]$ ,  $\mathbf{E}^\omega \parallel [1\bar{1}0]$ , and  $\mathbf{H} \parallel [1\bar{1}0]$  configuration, where  $\mathbf{k}^\omega \cdot (\mathbf{P} \times \mathbf{M}) \neq 0$ ,  $\mathbf{P}_H^\omega$  is parallel to  $\mathbf{P}_E^\omega$  and directional dichroism is actually observed [14]; in contrast, in the  $\mathbf{k}^\omega \parallel [001]$ ,  $\mathbf{H}^\omega \parallel [110]$ ,  $\mathbf{E}^\omega \parallel [1\bar{1}0]$ , and

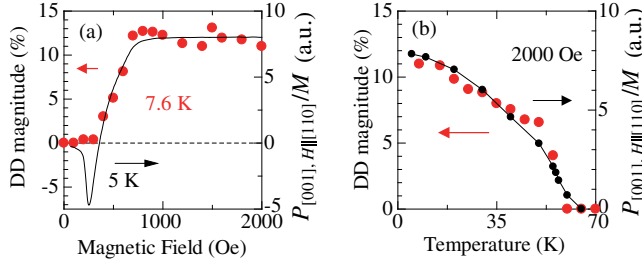


FIG. 4 (color online). Magnetic-field (a) and temperature (b) dependence of the magnitude of the directional dichroism measured under the  $\mathbf{k}||\mathbf{H}||[100]$  configuration at 7.6 K (closed circles). The variation of  $P_{[001],H||[110]}/M$  is also presented for comparison, in which  $P_{[001],H||[110]}$  and  $M$  are measured under  $\mathbf{H}||[110]$  and  $\mathbf{H}||[001]$ , respectively, at 5 K. The temperature dependences in (b) are measured at  $H = 2000$  Oe.

$\mathbf{H}||[1\bar{1}0]$  configuration, where  $\mathbf{k}^\omega \cdot (\mathbf{P} \times \mathbf{M}) = 0$ ,  $\mathbf{P}_H^\omega$  is perpendicular to  $\mathbf{P}_E^\omega$  and, in fact, directional dichroism does not occur [14]. In this way, the interference between  $\mathbf{P}_H^\omega$  and  $\mathbf{P}_E^\omega$  can account for the directional dichroism irrespective of whether one has Faraday or Voigt geometries.

Because the interference between  $\mathbf{P}_H^\omega$  and  $\mathbf{P}_E^\omega$  (and equivalently between  $\mathbf{M}_H^\omega$  and  $\mathbf{M}_E^\omega$ ) plays a major role in the directional dichroism, the magnetic-field and temperature dependence of the directional-dichroism magnitude should be well reproduced in terms of  $\mathbf{P}_H^\omega$ . To address this issue, we define the magnitude of the directional dichroism as the nonreciprocal absorption divided by the reciprocal absorption and consider the geometry of Fig. 2(a). The reciprocal absorption is proportional to  $\chi^{\leftrightarrow \text{nm}}$  and hence to  $M_H^\omega$  [33]. As shown in Fig. 2(a),  $M_H^\omega$  can be viewed as a variation of  $\mathbf{M}$  under a rotating magnetic field around the [001] axis; therefore,  $M_H^\omega$  is proportional to the  $\mathbf{M}$  amplitude  $M$ . Likewise, the nonreciprocal absorption is proportional to  $\chi^{\leftrightarrow \text{em}}$  and hence to  $P_H^\omega$  [34]. We can estimate  $P_H^\omega$  from the behavior of  $\mathbf{P}$  under a rotating magnetic field, which has already been reported in Ref. [24]. In the literature, the [001] component of  $\mathbf{P}$  shows sinusoidal behavior under a rotating magnetic field around the [001] axis; therefore,  $P_H^\omega$  in the geometry of Fig. 2(a) is found to be proportional to the [001] component of  $\mathbf{P}$  under  $\mathbf{H}||[110]$ ,  $P_{[001],H||[110]}$ . Eventually, we can find that the magnitude of the directional dichroism is proportional to  $P_{[001],H||[110]}/M$ .

In Fig. 4(a), we summarize the magnetic-field dependences of (i) the directional-dichroism magnitude, which is experimentally characterized as  $[(\Delta S_{12} - \Delta S_{21}) / \frac{1}{2}(\Delta S_{12} + \Delta S_{21})]$ , in the  $\mathbf{k}^\omega||\mathbf{H}||[100]$  configuration and (ii)  $P_{[001],H||[110]}/M$ , where  $P_{[001],H||[110]}$  and  $M$  were recorded under  $\mathbf{H}||[110]$  and  $\mathbf{H}||[001]$ , respectively: The temperature dependences of (i) and (ii) are also shown in Fig. 4(b).  $P_{[001],H||[110]}/M$  well reproduces the overall features of the directional-dichroism magnitude in both

the magnetic-field and temperature dependences except for the sharp dip seen in the magnetic-field dependence of  $P_{[001],H||[110]}/M$  [Fig. 4(a)], again indicating a key role of the  $\mathbf{P}_E^\omega$ - $\mathbf{P}_H^\omega$  interference in the directional dichroism.

Up to this point, we have focused on a system such that the ME coupling is given explicitly. Now, we consider the directional dichroism in a system with an arbitrary form of ME coupling. Without loss of generality, we can set  $\mathbf{k}^\omega||\mathbf{y}$ ,  $\mathbf{H}^\omega||\mathbf{z}$ , and  $\mathbf{E}^\omega||\mathbf{x}$ . The  $x$  component of  $\mathbf{P}_H^\omega$  (denoted as  $P_{H,x}^\omega$ ), which couples with the microwave  $\mathbf{E}^\omega$  ( $||\mathbf{x}$ ) and causes the directional dichroism, can be approximated as

$$P_{H,x}^\omega \simeq \frac{\partial P_x}{\partial H_z} H_z^\omega = \left( \cos \theta \frac{\partial P_x}{\partial H} - \frac{\sin \theta}{H} \frac{\partial P_x}{\partial \theta} \right) H_z^\omega. \quad (4)$$

Here,  $H$ ,  $\phi$ , and  $\theta$  are the radial distance, azimuth angle, and polar angle, respectively, with respect to  $\mathbf{H}$  in conventional polar coordinates. Three archetypal geometries are given as (i)  $\phi = \theta = \pi/2$ , i.e., Faraday geometry with  $\mathbf{H}||\mathbf{y}$  and  $\mathbf{H} \perp \mathbf{H}^\omega$ , (ii)  $\phi = 0$  and  $\theta = \pi/2$ , i.e., Voigt geometry with  $\mathbf{H}||\mathbf{x}$  and  $\mathbf{H} \perp \mathbf{H}^\omega$ , and (iii)  $\theta = 0$ , i.e., Voigt geometry with  $\mathbf{H}||\mathbf{z}$  and  $\mathbf{H}||\mathbf{H}^\omega$ . In the case of  $\mathbf{H} \perp \mathbf{H}^\omega$ , what determines the magnitude of the directional dichroism is common between Faraday and Voigt geometries and given as  $P_{H,x}^\omega = -(1/H)(\partial P_x / \partial \theta) H_z^\omega$ , i.e., a variation in  $P_x$  when the  $\mathbf{H}$  direction is slightly slanted from the original axis. In contrast, in the case of (iii), the magnetic-field dependence of  $P_x$ , i.e.,  $\partial P_x / \partial H$ , determines the directional dichroism. Equation (4) thus indicates that a dominant factor of the directional-dichroism magnitude depends on the magnetic-resonance mode; for instance,  $\partial P_x / \partial \theta$  is dominant in the Skyrmion counterclockwise rotational mode as well as the magnetic resonance in the ferrimagnetic phase, whereas  $\partial P_x / \partial H$  for the Skyrmion breathing mode [14]. In most cases, the ME resonance requires the  $\mathbf{H} \perp \mathbf{H}^\omega$  condition; the consideration of  $\partial P_x / \partial \theta$  can hence give a guideline for achieving the largest directional dichroism in a given material.

In conclusion, we have successfully observed microwave directional dichroism in Faraday geometry in the multiferroic chiral helimagnet  $\text{Cu}_2\text{OSeO}_3$ . To the best of our knowledge, this is the first observation of directional dichroism in Faraday geometry, often called magnetochiral dichroism, in the microwave-frequency range. We found that the directional dichroism arises from an interference between the microwave- $\mathbf{H}^\omega$ -induced electric polarization and the microwave- $\mathbf{E}^\omega$ -induced electric polarization. Our results establish the clear case that magnetoelectric coupling in the dc regime can account for directional dichroism accompanying magnetoelectric resonance at microwave frequencies.

The authors thank Y. Takahashi, M. Mochizuki, Y. Onose, and T. Kurumaji for enlightening discussions. This work was supported by the Grant-in-Aid for Scientific

Research (Grants No. 24224009, No. 24226002, and No. 26610109) from the JSPS and the Funding Program in World-Leading Innovative R&D on Science and Technology (FIRST Program).

*Note added in proof.*—We have recently become aware of a theoretical calculation on the microwave magnetochiral dichroism in  $\text{Cu}_2\text{OSeO}_3$  in Ref. [35]. Our experiment and the theory show a good agreement.

---

\*Present address: Technology and Business Development Unit, Murata Manufacturing Co., Ltd., Nagaokakyo, Kyoto 617-8555, Japan.

- [1] T. Kimura, T. Goto, H. Shintani, K. Ishizaka, T. Arima, and Y. Tokura, *Nature (London)* **426**, 55 (2003).
- [2] W. Eerenstein, N. D. Mathur, and J. F. Scott, *Nature (London)* **442**, 759 (2006).
- [3] S.-W. Cheong and M. Mostovoy, *Nat. Mater.* **6**, 13 (2007).
- [4] Y. Tokura, S. Seki, and N. Nagaosa, *Rep. Prog. Phys.* **77**, 076501 (2014).
- [5] Y. Yamasaki, S. Miyasaka, Y. Kaneko, J.-P. He, T. Arima, and Y. Tokura, *Phys. Rev. Lett.* **96**, 207204 (2006).
- [6] Y. Tokunaga, N. Furukawa, H. Sakai, Y. Taguchi, T. Arima, and Y. Tokura, *Nat. Mater.* **8**, 558 (2009).
- [7] Y. S. Chai, S. Kwon, S. H. Chun, I. Kim, B.-G. Jeon, K. H. Kim, and S. Lee, *Nat. Commun.* **5**, 4208 (2014).
- [8] A. Pimenov, A. A. Mukhin, V. Yu. Ivanov, V. D. Travkin, A. M. Balbashov, and A. Loidl, *Nat. Phys.* **2**, 97 (2006).
- [9] N. Kida, D. Okuyama, S. Ishiwata, Y. Taguchi, R. Shimano, K. Iwasa, T. Arima, and Y. Tokura, *Phys. Rev. B* **80**, 220406 (2009).
- [10] S. Seki, N. Kida, S. Kumakura, R. Shimano, and Y. Tokura, *Phys. Rev. Lett.* **105**, 097207 (2010).
- [11] Y. Takahashi, R. Shimano, Y. Kaneko, H. Murakawa, and Y. Tokura, *Nat. Phys.* **8**, 121 (2011).
- [12] I. Kezsmárki, N. Kida, H. Murakawa, S. Bordacs, Y. Onose, and Y. Tokura, *Phys. Rev. Lett.* **106**, 057403 (2011).
- [13] S. Bordács, I. Kézsmárki, D. Szallár, L. Demkó, N. Kida, H. Murakawa, Y. Onose, R. Shimano, T. Rőöm, U. Nagel, S. Miyahara, N. Furukawa, and Y. Tokura, *Nat. Phys.* **8**, 734 (2012).
- [14] Y. Okamura, F. Kagawa, M. Mochizuki, M. Kubota, S. Seki, S. Ishiwata, M. Kawasaki, Y. Onose, and Y. Tokura, *Nat. Commun.* **4**, 2391 (2013).
- [15] Y. Takahashi, Y. Yamasaki, and Y. Tokura, *Phys. Rev. Lett.* **111**, 037204 (2013).
- [16] I. Kézsmárki, N. Szallár, S. Bordács, H. Murakawa, Y. Tokura, H. Engelkamp, T. Rőöm, and U. Nagel, *Nat. Commun.* **5**, 3203 (2014).
- [17] S. Kibayashi, Y. Takahashi, S. Seki, and Y. Tokura, *Nat. Commun.* **5**, 4583 (2014).
- [18] N. A. Spaldin, M. Fiebig, and M. Mostovoy, *J. Phys. Condens. Matter* **20**, 434203 (2008).
- [19] G. L. Rikken and E. Raupach, *Nature (London)* **390**, 493 (1997).
- [20] J.-W. G. Bos, C. V. Colin, and T. T. M. Palstra, *Phys. Rev. B* **78**, 094416 (2008).
- [21] M. Belesi, I. Rousochatzakis, H. C. Wu, H. Berger, I. V. Shvets, F. Mila, and J. P. Ansermet, *Phys. Rev. B* **82**, 094422 (2010).
- [22] S. Seki, X. Z. Yu, S. Ishiwata, and Y. Tokura, *Science* **336**, 198 (2012).
- [23] T. Adams, A. Chacon, M. Wagner, A. Bauer, G. Brandl, B. Pedersen, H. Berger, P. Lemmens, and C. Pfleiderer, *Phys. Rev. Lett.* **108**, 237204 (2012).
- [24] S. Seki, S. Ishiwata, and Y. Tokura, *Phys. Rev. B* **86**, 060403 (2012).
- [25] See Supplemental Material at <http://link.aps.org/supplemental/10.1103/PhysRevLett.114.197202> for supplemental data and the analysis procedure.
- [26] Y. Onose, Y. Okamura, S. Seki, S. Ishiwata, and Y. Tokura, *Phys. Rev. Lett.* **109**, 037603 (2012).
- [27] M. Kataoka, *J. Phys. Soc. Jpn.* **56**, 3635 (1987).
- [28] For simplicity, we assume an isotropic  $\chi^{\text{mm}}$ , but slight anisotropy does not change our conclusion so much.
- [29] C. Jia, S. Onoda, N. Nagaosa, and J.-H. Han, *Phys. Rev. B* **76**, 144424 (2007).
- [30] T. Arima, *J. Phys. Soc. Jpn.* **76**, 073702 (2007).
- [31] M. Mochizuki and S. Seki, *Phys. Rev. B* **87**, 134403 (2013).
- [32] The theoretical model well reproduces the experimental results except for a helical spin state with multiple  $q$ -vector domains. For more details, see Ref. [24].
- [33] A. G. Gurevich and G. A. Melkov, *Magnetization Oscillations and Waves* (CRC Press, Boca Raton, 1996).
- [34] D. Szallár, S. Bordács, V. Kocsis, T. Room, U. Nagel, and I. Kezsmárki, *Phys. Rev. B* **89**, 184419 (2014).
- [35] M. Mochizuki, *Phys. Rev. Lett.* **114**, 197203 (2015).